

Electronic Supplementary Information (ESI)

Insight into the Ga/In flux ratio and crystallographic plane dependence for MBE assembly growth of InGaN nanorods on patterned sapphire substrates

Jian Shen,^{‡a b d} Yuefeng Yu,^{‡a c} Jia Wang,^d Yulin Zheng,^{a c} Yang Gan,^{* b} Guoqiang Li^{* a c}

^a State Key Laboratory of Luminescent Materials and Devices, South China University of Technology, Guangzhou 510640, China.

^b School of Chemistry and Chemical Engineering, Harbin Institute of Technology, Harbin 150001, China.

^c Engineering Research Center on Solid-State Lighting and its Informationisation of Guangdong Province, South China University of Technology, Guangzhou 510640, China.

^d Center for Integrated Research of Future Electronics, and Institute of Materials and Systems for Sustainability, Nagoya University, Nagoya 464-8601, Japan

[‡]These authors contributed equally.

*Corresponding author, E-mail: ygan@hit.edu.cn and msgli@scut.edu.cn.

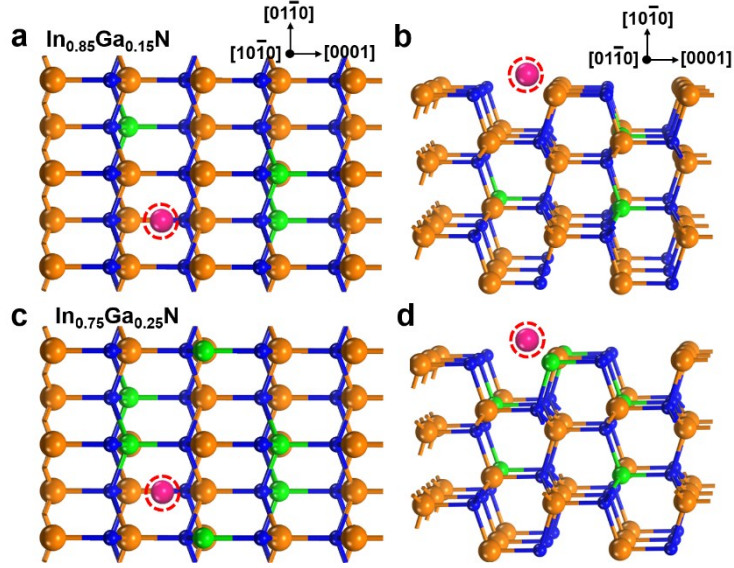


Fig. S1 The simulated top-view and side-view schematic illustrations of the (100) plane of (a) and (b) $\text{In}_{0.85}\text{Ga}_{0.15}\text{N}$, (c) and (d) $\text{In}_{0.75}\text{Ga}_{0.25}\text{N}$.

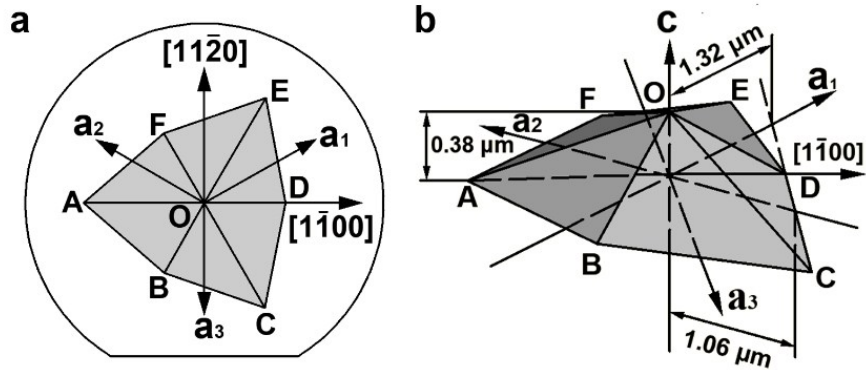


Fig. S2 (a) The constructed hexagonal pyramid (OABCDEF) on the c -plane sapphire wafer with known crystallographic orientations of $[1\ 1\ 0]$ and $[1\ 0\ 0]$. (b) A model hexagonal pyramid with a hexagonal coordinate system for determining intercepts of C_3 -plane on a_1 -, a_2 -, and c -axes.

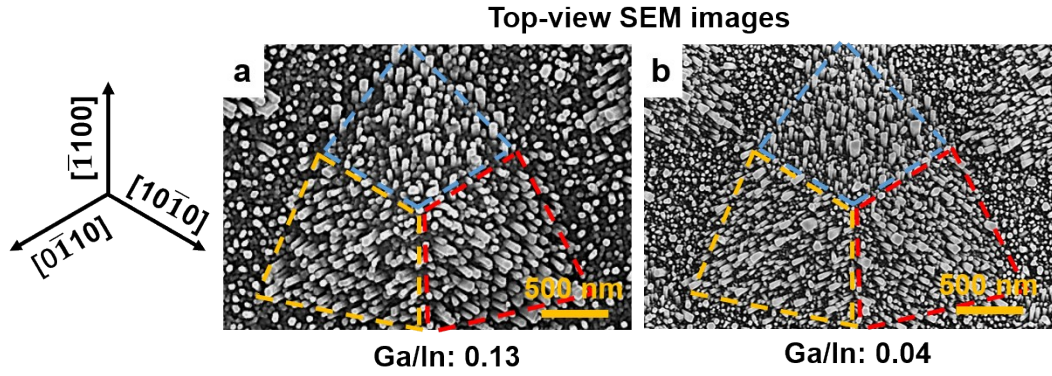


Fig. S3 The inclination and corresponding projected crystallographic orientation of InGaN NRs on C_3 -planes of hexagonal pyramids grown with the Ga/In flux ratio of (a) 0.13 and (b) 0.04 in top-view SEM images.

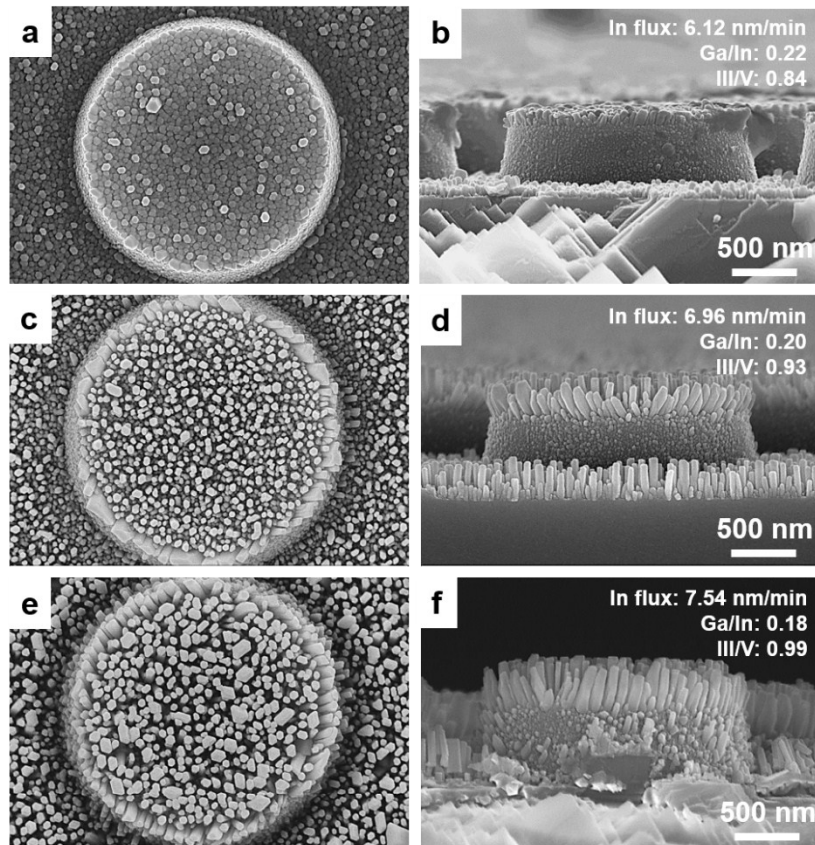


Fig. S4 Top-view and side-view SEM images of InGaN compact layers and NRs grown on faceted cylinder PSS with varying In flux of (a) and (b) 6.12 nm/min, (c) and (d) 6.96 nm/min, (e) and (f) 7.54 nm/min.

Fig. S5(a) shows the PL spectrum of InGaN NRs grown with varying Ga/In flux ratio (0.04–0.33). The PL spectral peak positions of InGaN samples with Ga/In flux ratio of 0.33, 0.22, 0.13, and 0.04, are determined to be 771.1 nm, 794.7 nm, 854.7 nm, and 912.9 nm, respectively. Then, the bandgap of InGaN samples with Ga/In flux ratio of 0.33, 0.22, 0.13, and 0.04, are determined to be 1.61 eV, 1.56 eV, 1.45 eV, and 1.36 eV, respectively. It is well accepted that the bandgap of $\text{In}_{(1-x)}\text{Ga}_x\text{N}$ can be well fitted by the following standard bowing equation¹⁻³:

$$E_g(\text{In}_{1-x}\text{Ga}_x\text{N}) = xE_g(\text{GaN}) + (1-x)E_g(\text{InN}) - bx(1-x)$$

For $\text{In}_{(1-x)}\text{Ga}_x\text{N}$ nanowire model, the corresponding parameters have been determined: $E_g(\text{GaN}) = 3.43$ eV; $E_g(\text{InN}) = 1.12$ eV; $b = 1.01$ eV.¹ In this model, $E_g(\text{InN})$ of 1.12 eV was employed instead of the 0.7 eV value in recent reports². A proposed explanation of the disparate results is that there is a dependence of the bandgap on the free-electron concentration⁴. Based on the chemical composition of InGaN NRs determined by EDXS and HRTEM characterizations, it can be found that the relationship among PL peak position, bandgap, and composition of as-obtained InGaN NRs in our works corresponds well with the reported bowing equation of InGaN nanowire model.¹ Therefore, based on the known bandgap and PL spectral peak position, using standard bowing equation, the component of InGaN NRs with the Ga/In flux ratio of 0.33, 0.22, 0.13, and 0.04, is then determined as $\text{In}_{0.69}\text{Ga}_{0.31}\text{N}$, $\text{In}_{0.72}\text{Ga}_{0.28}\text{N}$, $\text{In}_{0.78}\text{Ga}_{0.22}\text{N}$, and $\text{In}_{0.84}\text{Ga}_{0.16}\text{N}$, respectively, which is similar to the EDXS result.

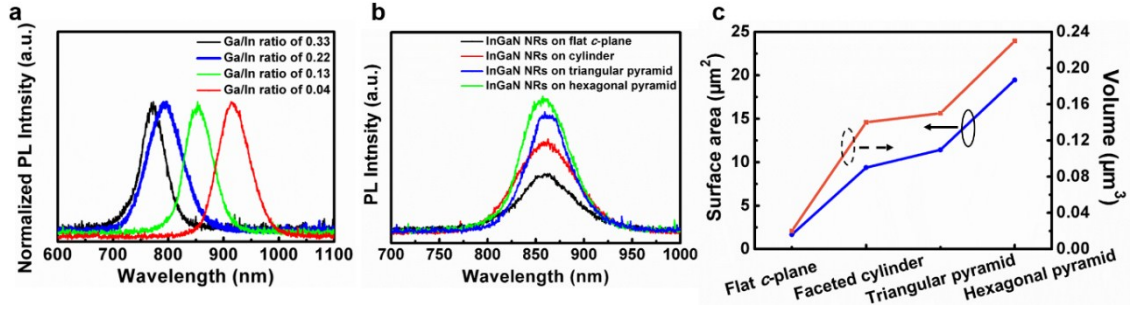


Fig. S5 (a) Room temperature PL spectrum of InGaN samples grown with Ga/In ratio of 0.33, 0.22, 0.13, and 0.04. (b) Room temperature PL spectrum, and (b) surface area and volume of InGaN NRs (over a $1.0 \times 1.0 \mu\text{m}^2$ projected area) with the Ga/In flux ratio of 0.13 on flat *c*-plane substrate, faceted cylinder with curved C_0 -zone and top *c*-plane, triangular pyramid with rough C_2 -plane, as well as hexagonal pyramid with C_3 -plane.

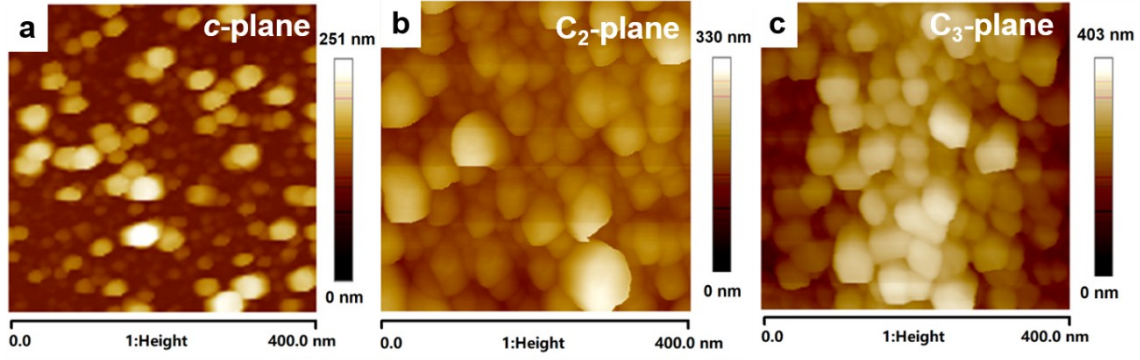


Fig. S6 AFM plane-view images of InGaN nucleated islands grown with the Ga/In flux ratio of 0.13 and the growth time of 15 min on (a) *c*-plane, (b) C_2 -plane, and (c) C_3 -plane.

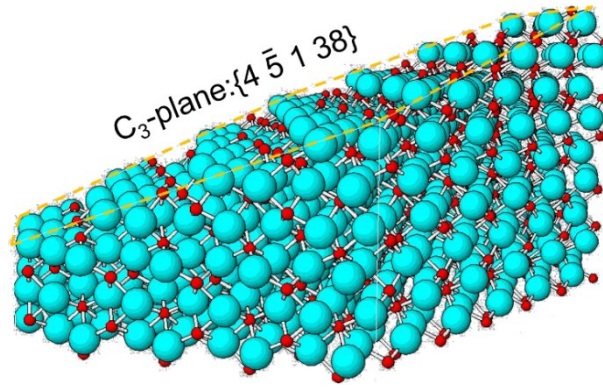


Fig. S7 Simulated atom arrangement in the step-terrace structures of C_3 -plane of high Miller index ($\{4 \ 1 \ 38\}$).

Table S1 Analysis of the Ga, In, N fluxes, and the determination of Ga/In, III/V, Ga/N flux ratios in growth condition. Analysis of the In-contents in InGaN NRs determined by PL and EDXS, as well as calculated by the effective In and Ga fluxes.

Ga flux (nm/min)	In flux (nm/min)	N flux (nm/min)	Ga/In ratio	III/V ratio	Ga/N ratio	In-content from PL	In-content from EDXS	Calculated In-content
2.01	6.12	8.97	0.33	0.91	0.22	0.69	0.67	0.75
1.37	6.12	8.97	0.22	0.84	0.15	0.72	0.71	0.81
0.79	6.12	8.97	0.13	0.77	0.08	0.78	0.77	0.89
0.27	6.12	8.97	0.04	0.71	0.03	0.84	0.85	0.96

Table S1 reveals the difference of experimentally determined In-contents (PL and EDXS) and calculated In-contents ($x_{In} = In_{eff} / (In_{eff} + Ga_{eff})$) from the determined effective In/Ga fluxes (In_{eff} and Ga_{eff}). The calculated In-contents from effective Ga/In fluxes is based on the precondition of complete incorporation of In and Ga. It can be found that the measured In-

contents in InGaN are 8%–12% lower than calculated In-contents. As reported, the In flux can be completely incorporated at the growth temperature below 500°C, and the In-content in InGaN continuously decreases as growth temperature increases from 500°C to 700°C due to the In desorption.^{5, 6} The significant In-content decrease of 10% can be found at higher growth temperature of 565–580°C⁵ and 575–600°C⁶. Therefore, the In-content decrease of 8%–12% at the higher growth temperature of 576–579°C than that below 500°C (for the case of complete incorporation) can be confidently attributed to the measurable In desorption.

References

- 1 T. Kuykendall, P. Ulrich, S. Aloni and P. J. N. m. Yang, *Nat. Mater.*, 2007, **6**, 951-956.
- 2 J. Wu, *J. Appl. Phys.*, 2009, **106**, 011101.
- 3 J. Wu, W. Walukiewicz, K. M. Yu, J. Ager III, E. Haller, H. Lu and W. Schaff, *Appl. Phys. Lett.*, 2002, **80**, 4741-4743.
- 4 J. Wu, W. Walukiewicz, W. Shan, K. Yu, J. Ager III, E. Haller, H. Lu and W. Schaff, *Phys. Rev. B*, 2002, **66**, 201403.
- 5 R. Averbeck and H. Riechert, *Phys. Stat. Sol.*, 1999, **176**, 301-305.
- 6 I. Stanley, G. Coleiny and R. Venkat, *J. Cryst. Growth*, 2003, **251**, 23-28.